AD-A098 834 NAVAL RESEARCH LAB WASHINGTON DC F/G 17/9
PRELIMINARY STUDY OF REJECTING TARGETLIKE INTERFERENCE IN RADAR--ETC(U)
MAY 81 B H CANTRELL
UNCLASSIFIED NRL-8472 NL

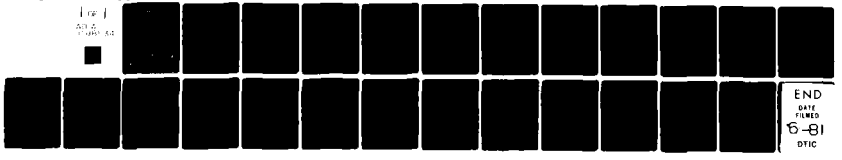

END
DATE FILMED
6-81
DTIC

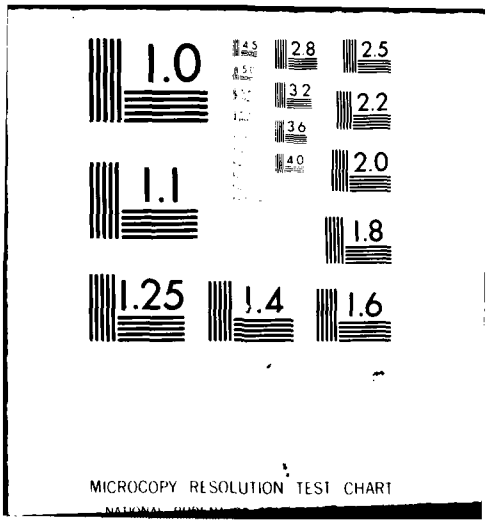
1.0
1.1
1.25
1.4
1.6
1.8
2.0
2.2
2.5
2.8
3.2
3.6
4.0
MICROCOPY RESOLUTION TEST CHART

NRL Report 8472

Preliminary Study of Rejecting Targetlike Interference in Radar

B. H. CANTRELL

Radar Analysis Branch
Radar Division

May 11, 1981

NAVAL RESEARCH LABORATORY
Washington, D.C.

UNCLASSIFIED

SECURITY CLASSIFICATION OF THIS PAGE (When Data Entered)

REPORT DOCUMENTATION PAGE	READ INSTRUCTIONS BEFORE COMPLETING FORM
1. REPORT NUMBER: NRL Report 8472	2. GOVT ACCESSION NO.: AD-A098834
3. RECIPIENT'S CATALOG NUMBER	
4. TITLE (and Subtitle): PRELIMINARY STUDY OF REJECTING TARGETLIKE INTERFERENCE IN RADAR	5. TYPE OF REPORT & PERIOD COVERED: Interim Report on a continuing NRL problem
	6. PERFORMING ORG. REPORT NUMBER
7. AUTHOR(s): B. H. Cantrell	8. CONTRACT OR GRANT NUMBER(s)
9. PERFORMING ORGANIZATION NAME AND ADDRESS: Naval Research Laboratory, Washington, DC 20375	10. PROGRAM ELEMENT, PROJECT, TASK AREA & WORK UNIT NUMBERS: 61153N; RR0210541; NRL Problem 53-0626-0-1
11. CONTROLLING OFFICE NAME AND ADDRESS: Office of Naval Research, Arlington, VA 22217	12. REPORT DATE: May [redacted]81
	13. NUMBER OF PAGES: 24
14. MONITORING AGENCY NAME & ADDRESS(if different from Controlling Office)	15. SECURITY CLASS. (of this report): UNCLASSIFIED
	15a. DECLASSIFICATION/DOWNGRADING SCHEDULE

16. DISTRIBUTION STATEMENT (of this Report)

Approved for public release; distribution unlimited.

17. DISTRIBUTION STATEMENT (of the abstract entered in Block 20, if different from Report)

18. SUPPLEMENTARY NOTES

19. KEY WORDS (Continue on reverse side if necessary and identify by block number)

Interference rejection
Signal processing
Radar
Detection

20. ABSTRACT (Continue on reverse side if necessary and identify by block number)

A means of detecting target echoes from targetlike interference in radars was studied. The procedure differed from the more conventional means of pulse-to-pulse coincidence detection by examining the fine structure of a single pulse. Two discriminants were postulated and their performance was evaluated using computer-generated data. The results look encouraging but because the fine structure which is sensitive to small changes is being used, real data are needed before the technique can be more fully assessed.

DD FORM 1 JAN 73 1473 EDITION OF 1 NOV 65 IS OBSOLETE
S/N 0102-014-6601

SECURITY CLASSIFICATION OF THIS PAGE (When Data Entered)

2511

CONTENTS

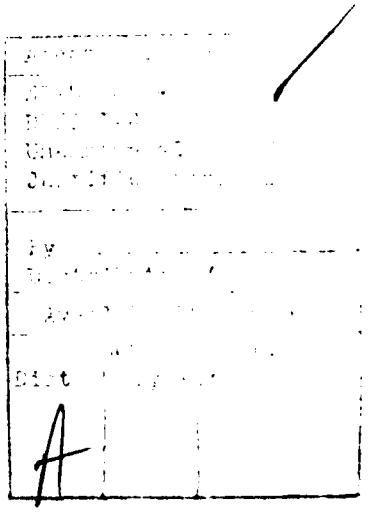

PRELIMINARY STUDY OF REJECTING TARGETLIKE INTERFERENCE IN RADAR

INTRODUCTION

The processing of radar signals has received considerable attention for a long time, and excellent results have been obtained in both practice and theory. The matched filter is an optimum means of detecting signals in noise, and many approximate implementations have been successfully constructed for a wide variety of problems. In radar the data are sometimes prewhitened by spatial filters such as sidelobe cancellers, mainlobe cancellers, and adaptive arrays. In the time or frequency domain, the prewhitening filters are MTI's and pulse doppler systems. The data are then passed through a matched filter (matched to the signal after prewhitening) to maximize the signal-to-noise ratio. Finally, the amplitude is compared to a threshold which may be locally generated to determine if a target has been detected.

The conventional processing works well as long as the data are or can be properly prewhitened and all that is of interest is target detections. However, in a radar, signals can appear to be targetlike but are not targets. For example, signals can be externally generated that appear nearly the same as echoes from radar targets and be received through both the antenna mainlobes and sidelobes. Furthermore, reflections can be obtained from undesirable reflectors other than targets such as land objects, rain, and a rough sea surface. A recent study showed how the echoes received by a radar could be classified into a number of categories [1]. The classification categories considered were land clutter, rain, noise jamming, thermal noise, short pulse interference, receiver saturation, and isolated targets. Most of these classifications depend upon looking at two consecutive echoes and using range cell-to-range cell examinations along with numbers computed from the signals in the local vicinity. The procedure worked quite well within the limits described. However, questions arose pertaining to whether more or better information could be extracted from the received radar signal by examining the fine structure of the radar echoes over short range intervals. Some benefits that might be derived could be the classification of targetlike signals on a single pulse as to whether the signal is interference or a true target echo, without using pulse coincidence detection. If this is possible, frequency agile operation could be used pulse-to-pulse and targetlike interference could be removed. Other benefits could come in the classification of signal types. It is the purpose of this study to examine the fine structure in radar signals over a small time interval for the purpose of classifying targets or interference. A number of signal classes will be generated and passed through a processor implemented on a computer that emulates a real time hardware device.

We first describe the simulation used in the study. Next, the spectrums of a wide variety of signals are given. Finally, two discriminants are formulated. One discriminant for testing the character of a received pulse is based on matching the spectral shape of the received signal to that of a stored replica obtained from a point target echo at essentially infinite signal-to-noise ratio. The other discriminant looks at the spectral symmetry about the carrier, or in other words, does the spectrum of the upper and lower sidebands match? Their performance is evaluated using several Monte Carlo runs.

Manuscript submitted January 21, 1981

DESCRIPTION OF STUDY PROCEDURE

The object of the subsequent development is to describe a means of obtaining a set of signals using simulation procedures and a way of discriminating between echoes from targets and other types of interference that look much like a target. We begin by considering a conventional receiver system.

Receiver System

A conventional superheterodyne receiver with in-phase and quadrature receiver channels is shown in Fig. 1. The IF or RF and low pass filters are implemented by using sampled data filters. The sampling rate is sufficiently high so that the difference equations used on the computer to simulate the filters are a very good approximation to actual filters described by differential equations. The 4th-order Chebishev filters with 1-dB ripple were chosen for both the IF and low pass filters. A frequency response of the receiver is shown in Fig. 2. This is obtained by using a sinusoidal source as the signal generator in Fig. 1 and determining the ratio of the peak amplitudes of the sinusoids in either the in-phase or quadrature channels to the input sinusoid.

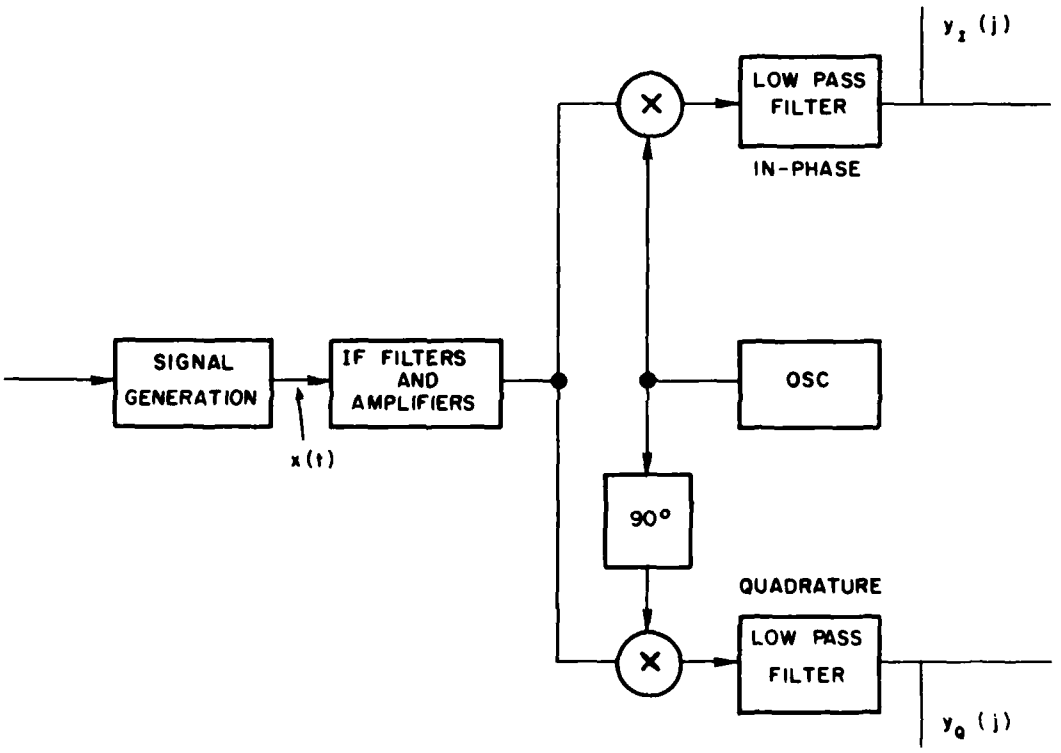

Fig. 1 — Block diagram of receiver

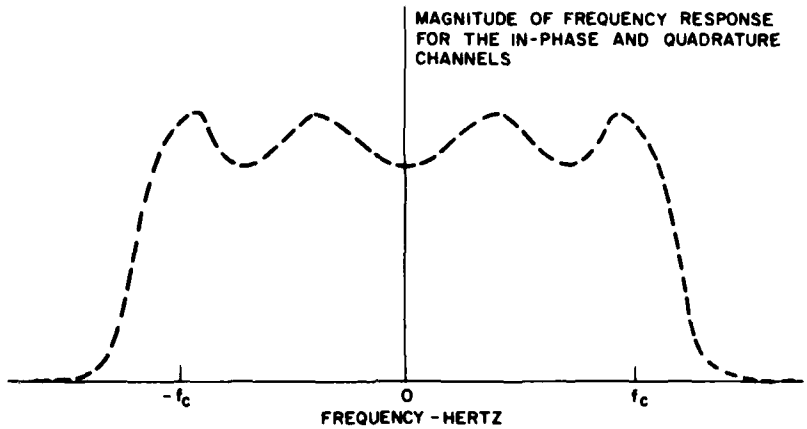

Fig. 2 — Frequency response of in-phase and quadrature channels $Y_I(i)$ and $Y_Q(i)$ respectively

Received Signal from Point Target

The transmitted radar signal is assumed to be a Gaussian shaped RF pulse and after reflection from a point target, the signal entering the receiver is given by

$$X(t) = A \exp\{-[2f_c(t-\tau)]^2\} \cos(\omega_0(t-\tau) + \phi),$$

where A is the amplitude, t is time, τ is the time delay, ϕ is an arbitrary phase shift including the phase shift due to doppler, ω_0 is the RF center frequency, f_c is the filter cut off frequency, and $X(t)$ is the signal generation output. The shape of this waveform after being passed through the receiver is shown in Fig. 3. The pulse waveform is the same for both the in-phase and quadrature channels except for amplitude which is proportional to the cosine and sine of carrier phase. The magnitude of the frequency response of this received signal is shown in Fig. 4 along with the receiver's frequency response. We see the filters are of wide enough bandwidth to pass most of the signal before sharp rejection in frequency occurs.

Sideband Operation

The signal was separated into both lower and upper sideband components for the following reason. Although the received signal from a point echo is a double sideband signal and, consequently, the

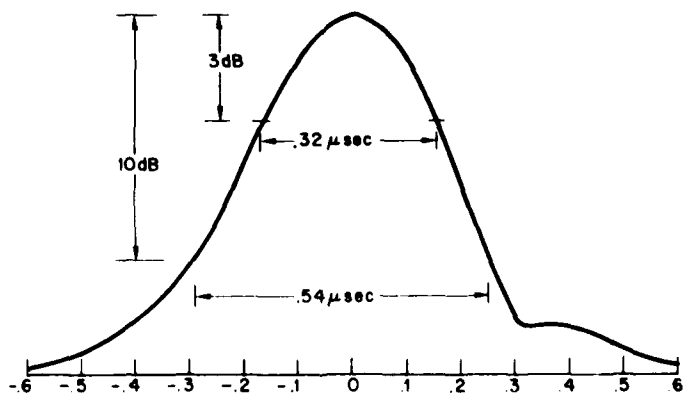

Fig. 3 — Pulse shape at baseband (time between samples of 0.1 μs)

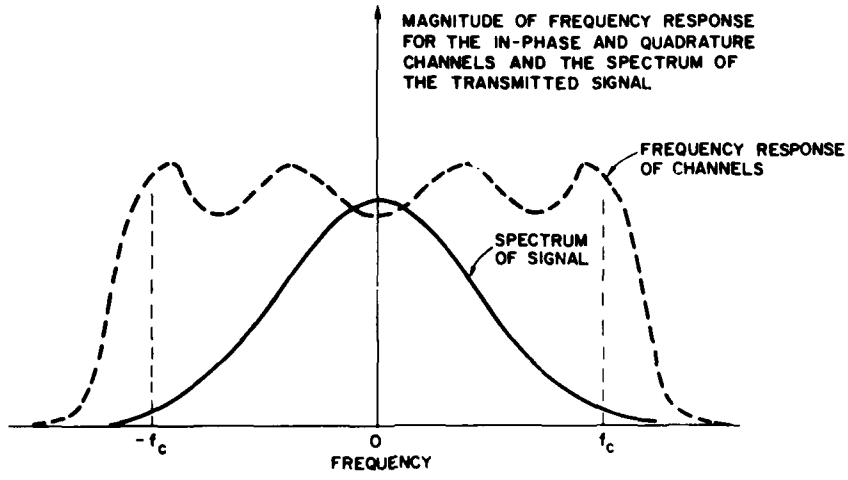

Fig. 4 — Frequency response of receiver and spectrum of signal

information above and below the carrier frequency is the same, interference may not have this characteristic. For example, an identical signal to the received radar echo but offset a little in carrier frequency may be received. If single sideband separation is not performed, the signals below and above the carrier are folded on top of one another and one cannot distinguish differences in signals above and below the carrier. For this reason the signal is separated into sidebands.

Because of the difficulty in separating the signal into sidebands by filtering at RF, a phase-shift method described in [2] was used. A block diagram of the operation is shown in Fig. 5. Note that the 90° phase shift in the quadrature channel is equivalent to the Hilbert transform in the frequency domain. The Fourier transform of the baseband signals is taken using 11 samples which basically covers the time interval over the time that a received pulse from a point target is present as shown in Fig. 3. For each new sample out of the filters the Fourier transform on the last 11 samples is taken using the equations

$$P_j(i) = \sum_{k=j}^{j+N-1} Y_I(k)\, e^{-\frac{ik2\pi\sqrt{-1}}{75}},$$

$$Q_j(i) = \sum_{k=j}^{j+N-1} Y_Q(k)\, e^{-\frac{ik2\pi\sqrt{-1}}{75}},$$

for $i = 0 \ldots M-1$ where $N = 11$ and $M = 16$. The formulas for computing the spectral lines are a direct application of the definition of the Fourier transform where the spectral spacing can be as close as desired. These formulas should not be confused with the discrete Fourier transform unless longer intervals and windowing are used to bring about equivalence. The formulas were set such that 15 frequencies are uniformly spaced within the passband of the filter at baseband. These can be implemented recursively by

$$P_{j+1}(i) = Y_I(j+1)\, e^{-\frac{i(j+1)2\pi\sqrt{-1}}{75}} + P_j(i) - Y_I(j-N)\, e^{-\frac{(j-N)i2\pi\sqrt{-1}}{75}},$$

and

$$Q_{j+1}(i) = Y_Q(j+1)\, e^{-\frac{i(j+1)2\pi\sqrt{-1}}{75}} + Q_j(i) - Y_Q(j-N)\, e^{-\frac{(j-N)i2\pi\sqrt{-1}}{75}}$$

Notice the new term is added to the old value of $P_j(i)$ or $Q_j(i)$ and the last value is subtracted. The implementation is shown in Fig. 6.

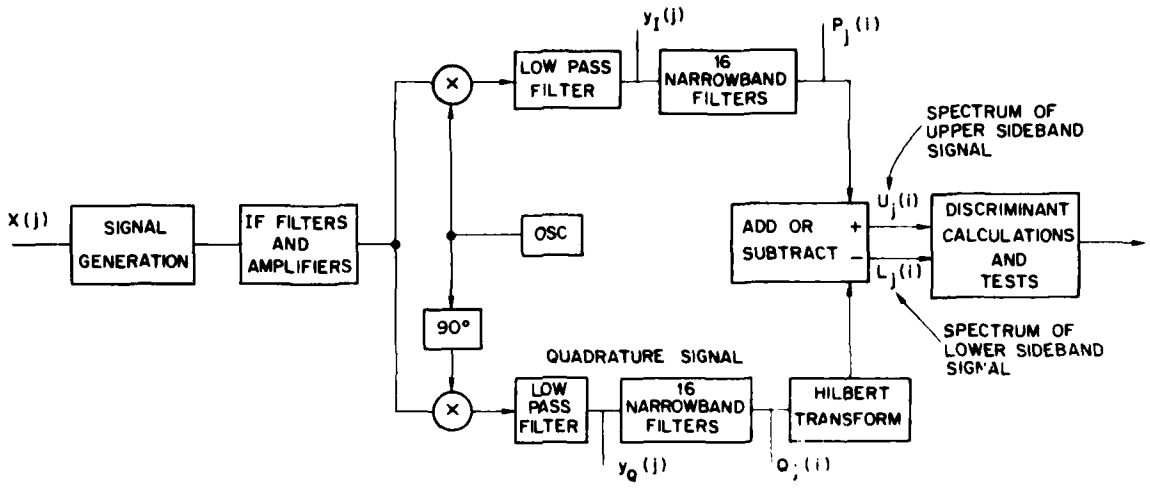

Fig. 5 — Block diagram of simulation

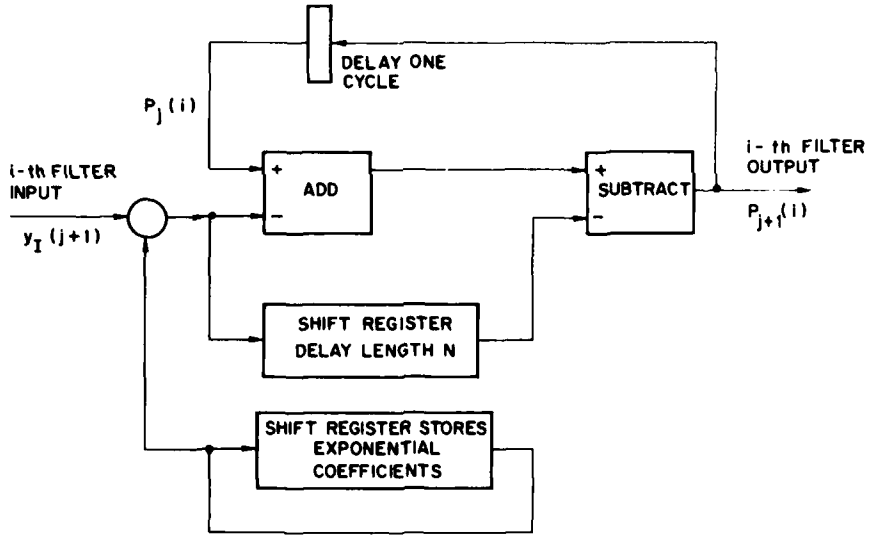

Fig. 6 — Means of implementing narrowband filters

Referring again to Fig. 5, the sideband separation from each new sample over the finite block of data consisting of 11 samples from both the in-phase and quadrature channel is completed as follows. After the signal is separated into 16 spectral lines across the passband in both the in-phase and quadrature channels, the Hilbert transform of the quadrature transformed signal is found. This is performed by multiplying the positive frequencies by the negative imaginary number, $-\sqrt{-1}$, and the negative frequencies by the positive imaginary number, $+\sqrt{-1}$. However, since the spectral lines of the positive and negative frequencies are mirror images, only the positive frequencies are used. The equations are:

$$U_j(i) = P_j(i) + \sqrt{-1}\, Q_j(i),$$

and

$$L_j(i) = P_j(i) - \sqrt{-1}\, Q_j(i).$$

Discriminants

The object is to require a signal received by the radar to match signals received from known targets as closely as possible in order to accept the signal as a real target echo. Conversely, the received signals that do not match the characteristics of target echoes are rejected as targets and declared to be interference. Some interference to be tested may only slightly differ from target echoes and may or may not be distinguishable on PPI or *A* scope presentations.

First let us consider the problems in matching an echo from a point target which is used as a reference. We find the amplitude, time of arrival, and the phase of the carrier are unknown. By normalizing the amplitude in both the in-phase and quadrature channels and time aligning the signal under test to the reference signal, a direct comparison of how well the signals match can be made. Alternately the carrier phase can be discarded by comparing normalized and time aligned envelope detected reference signals to those under test. However, we argued earlier that it may be worth while to consider both sidebands of the signals since some interference may be different in each sideband.

A problem occurs when the sideband separation is considered. In single sideband communications, the demodulator must be phase locked to the carrier to prevent distortion in the demodulated waveform. Since phase is never known we cannot separate the signal into the sidebands unless it is estimated. Rather than pursue the problems incurred by not knowing carrier phase, a means of comparing reference signals to signals under test that are independent of phase was studied. Furthermore, because of the problems in estimating time of arrival in the time domain only the frequency domain will be considered.

The way we chose to decide whether a target signal or interference signals are present is to compute discriminants based on the magnitude of the spectral lines. If the spectrum computation uses enough time samples to encompass the signal under test, the time of arrival becomes unimportant. Furthermore, the unknown phase information is not present in discriminants based on the magnitude of the spectral line. However, the magnitudes of the spectral lines must be normalized in amplitude. We begin by normalizing each computed spectral line by

$$\tilde{U}_j^2(i) = \frac{U_j(i)\ U_j^*(i)}{\frac{1}{N}\sum_{k=1}^{N} U_j(k)\, U_j^*(k)},$$

and

$$\tilde{L}_j^2(i) = \frac{L_j(i) L_j^*(i)}{\frac{1}{N}\sum_{k=1}^{N} L_j(k) L_j^*(k)},$$

where $\tilde{U}_j(i)$ and $\tilde{L}_j(i)$ are the normalized magnitude of the i th spectral line at the j th time sample of the spectral lines $U_j(i)$ and $L_j(i)$, respectively. Note that the phase is removed and each spectral line is normalized by the average power in the spectrum. We are also interested in the spectral shape when no noise is present. Consequently, we define

$$\bar{U}_j^2(i) = \tilde{U}_j^2(i) \text{ for no noise,}$$

and

$$\bar{L}_j^2(i) = \tilde{L}_j^2(i) \text{ for no noise,}$$

where $\bar{U}_j(i)$ and $\bar{L}_j(i)$ are the normalized spectral line heights when no noise is present for the i th spectral line and the jth time sample.

One discriminant for testing the character of a received pulse is based on matching the spectral shape of the received signal to that of a stored replica obtained from a point target echo at essentially infinite signal-to-noise ratio. The discriminant $\tilde{D}_j$ for the jth time sample is

$$\tilde{D}_j^2 = \frac{1}{2N} \sum_{k=1}^{N} [(\bar{U}_j(k) - \tilde{U}_j(k))^2 + (\bar{L}_j(k) - \tilde{L}_j(k))^2].$$

The discrimate computes the root-mean-square error between the normalized spectral lines and the stored replica. The other discriminant used looks at the spectral symmetry about the carrier, or in other words, do the spectrums of the upper and lower sidebands match? The discriminant is

$$\hat{D}^2(j) = \frac{1}{N} \sum_{k=1}^{N} (\tilde{U}_j(k) - \tilde{L}_j(k))^2.$$

This discriminant computes the root-mean-square error between the upper and lower sideband spectral lines. Both discriminants are finally averaged over five samples, which was found by trial and error. The new discriminants $\tilde{d}_j$ and $\hat{d}_j$ are defined as

$$\tilde{d}_j = \frac{1}{5} \sum_{k=1}^{5} \tilde{D}_k$$

and

$$\hat{d}_j = \frac{1}{5} \sum_{k=1}^{5} \hat{D}_k.$$

There exist other candidate discriminants that could be used in distinguishing between targets and interference; however, these were the only ones studied. Representative results are next discussed.

RESULTS FROM SIMULATION

The performance of the discriminants is studied in a qualitative manner for several reasons. First, the simulation used to obtain the results was fairly expensive, and the cost of obtaining substantial statistical results would have been prohibitive. Second, good target and transmit waveform models were not available, and it did not seem cost effective to study the particular discriminants in more depth until real data was obtained. Finally, a number of interference waveforms are considered but whether they are applicable to any one particular radars needs is unknown. Nevertheless, we will show qualitative results that should demonstrate the general nature of the performance one can expect.

Point Target Echoes

We begin by looking at results obtained from echoes from a point target 30 dB above thermal noise. Four trials are made and the results are shown in Figs. 7 and 8. Figure 7c shows the video as a function of time using an A scope presentation, and the echo is clearly visible above the thermal noise. The discriminants $\hat{d}_j$ and $\tilde{d}_j$ are shown over the same time record as the video. Again the position in time of the echo can easily be seen and occurs when the discriminants take on a value near zero. This means the upper and lower sideband spectrums closely match and they also match the reference spectrums as shown in Fig. 8b. The video in Fig. 8a is repeated from Fig. 7c for convenience. We note that both the upper and lower sideband spectrums in Fig. 8b are nearly Gaussian, like the reference spectrum shown in Fig. 4, and they match each other quite closely. The upper and lower sideband spectrums taken over a portion of the thermal noise is shown in Fig. 8c. There is considerable symmetry involved which is explained as follows. Both the upper and lower sideband spectrums are symmetric about the zero frequency. Furthermore, the spectrum that comes from the positive frequencies at RF is the mirror image of the spectrum that comes from the spectrum at negative frequencies at RF.

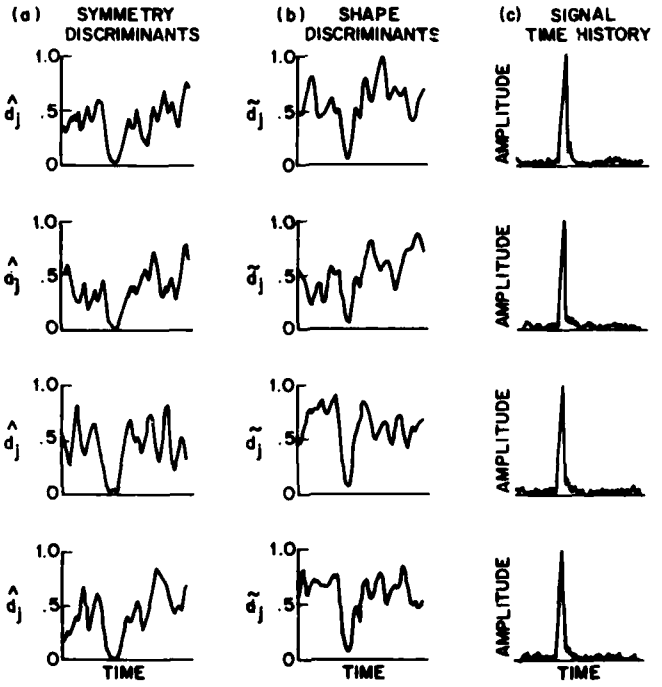

Fig. 7 — Time histories of discriminants and signals for four trials with a point target 30 dB above thermal noise

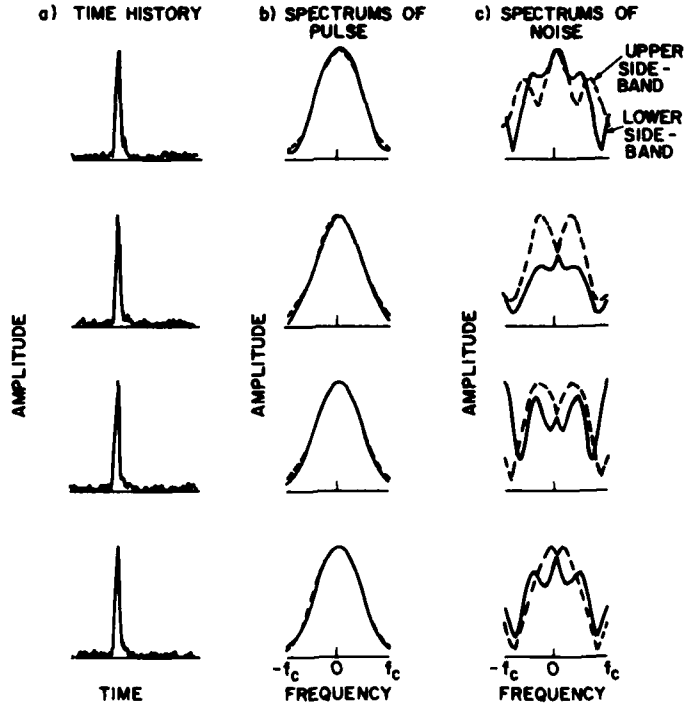

Fig. 8 — Time histories and spectrums of signals and noise for a point target 30 dB above thermal noise

We see that spectrums of thermal noise, as shown in Fig. 8c, are neither Gaussian shaped nor symmetric. Returning to Fig. 7a and b the discriminants take on a value near zero over the target echo and otherwise have high values. It appears, but is not demonstrated, that it is very difficult for a discriminant to take on a value near zero when only thermal noise is present. Figure 9 shows the same results as Fig. 7 except for a 20 dB signal-to-noise ratio. The major change is that the discriminants are not quite as close to zero when the target is present, which reflects the corruption on the spectrums by the increased relative noise level.

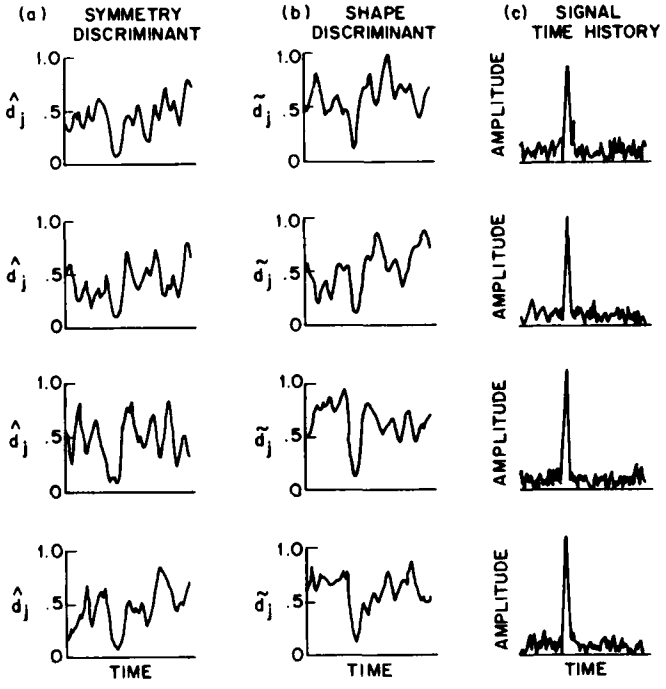

Fig. 9 — Time histories of discriminants and signals for four trials with a point target 20 dB above thermal noise

Interference

A number of signals designated as interference were passed through the receiver, and discriminants were computed. The results are shown in Figs. 10 through 26. The same signal used for obtaining the results shown in Fig. 7 was also used in Fig. 10 except that the carrier frequency was adjusted by an amount $0.2 \times f_t$ away from the carrier frequency. In comparing Figs. 7 and 10 we find that it is difficult to distinguish which signals are target echos and which ones are interference by looking at the A scope presentations in Figs. 7c and 10c. In addition, the discriminants in 7a and b and 10a and b take on values over a different range when the signal under test is present. However, the discriminants, when the interference is present, are not totally noiselike. The spectrums of the interference are shown in Fig. 11b and the video shown in Fig. 10c is repeated in Fig. 11a. We find the spectrum which is associated with the positive frequencies at RF is shifted up in frequency and the one with the negative frequencies at RF is shifted down in frequency and, consequently, the sidebands do not match nor is the spectrum Gaussian and centrally located. The results for the same case as shown in Fig. 10 is shown in Fig. 12 except 20 dB S/N was used. Reasonable discrimination was maintained.

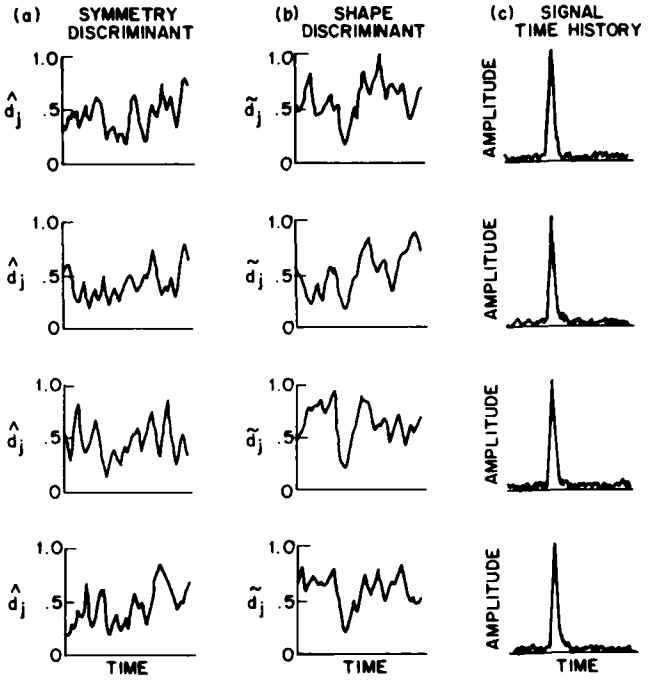

Fig. 10 — Time histories of discriminants and signals for four trials with a signal matching the transmitted signal but offset in frequency by 0.2 f_c (S/N = 30 dB)

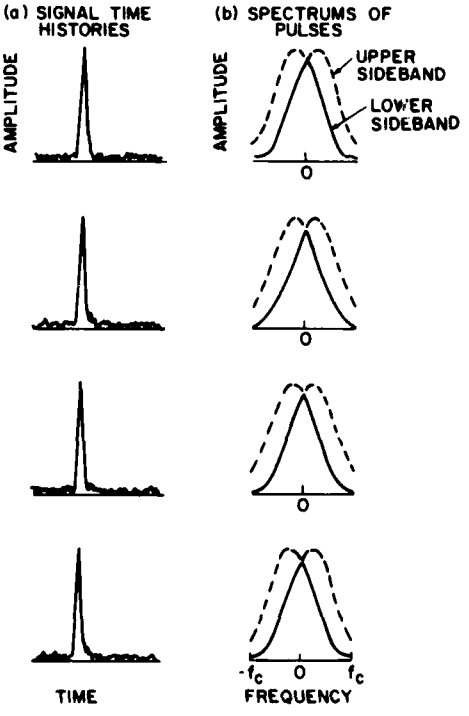

Fig. 11 — Time histories and spectrums of signal matching the transmitted signal but offset in frequency by 0.2 f_c (S/N = 30 dB)

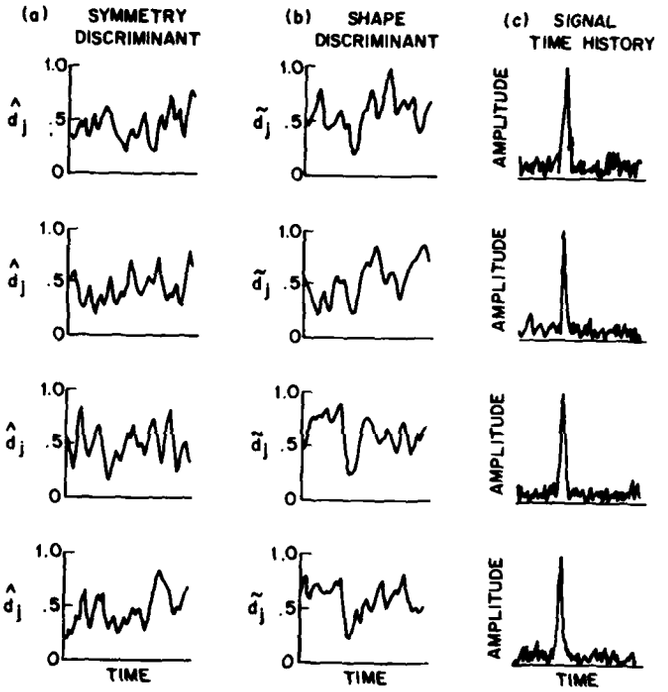

Fig. 12 — Time histories of discriminants and signals for four trials with a signal matching the transmitted signal but offset in frequency by 0.2 f_c (S/N = 20 dB)

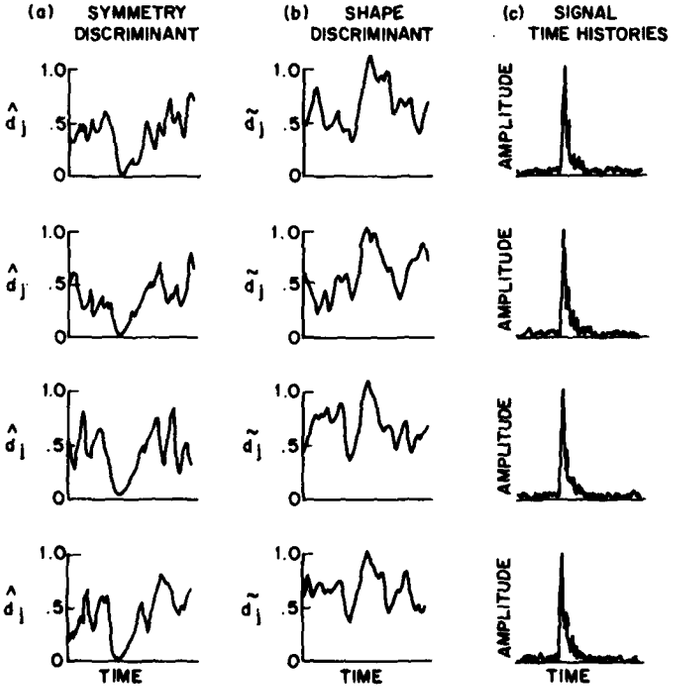

Fig. 13 — Time histories of discriminants and signals for four trials with a signal of bandwidth 5 × f_c and 30 dB above thermal noise

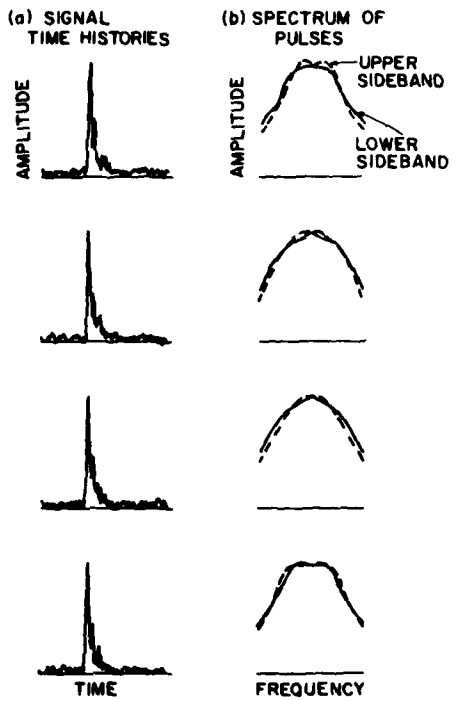

Fig. 14 — Time histories and spectrums of signals of bandwidth 5 × f_c and 30 dB above thermal noise

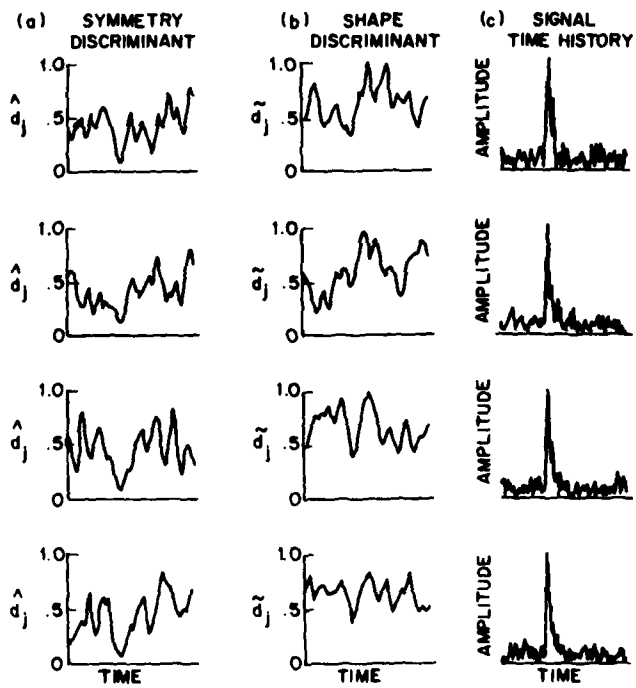

Fig. 15 — Time histories of discriminants and signals for four trials with a signal of bandwidth 5 × f_c and 20 dB above thermal noise

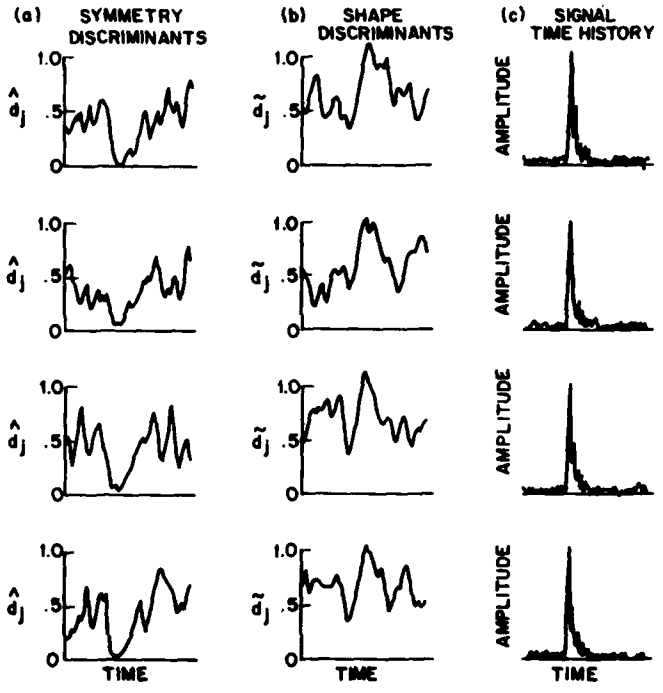

Fig. 16 — Time histories of discriminants and signals for four trials with a signal of bandwidth $5 \times f_c$, offset in frequency by $0.2 \times f_c$, and 30 dB above thermal noise

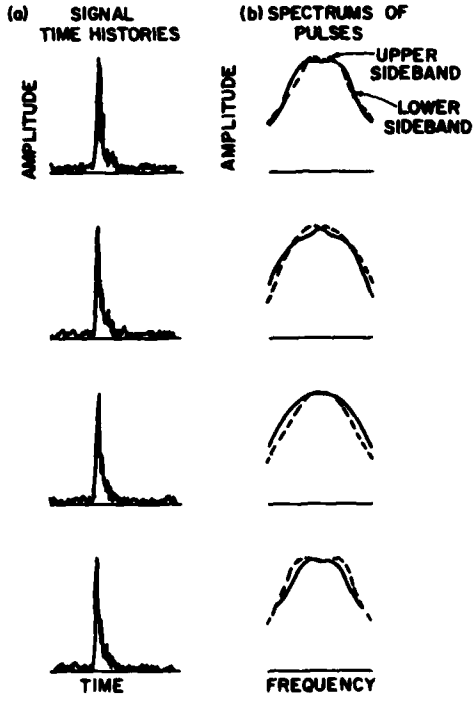

Fig. 17 — Time histories and spectrums of signals of bandwidths $5 \times f_c$, offset in frequency by $0.2 \times f_c$, and 30 dB above thermal noise

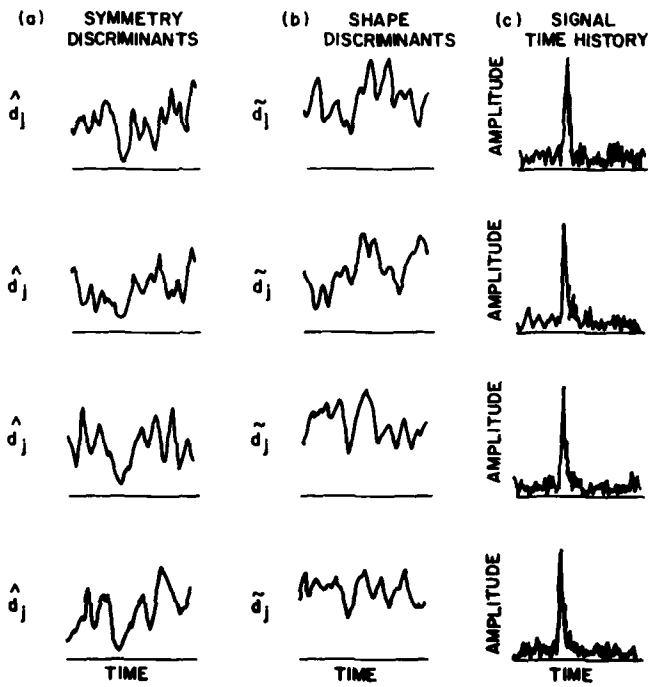

Fig. 18 — Time histories of discriminants and signals for four trials with a signal of bandwidth $5 \times f_c$, offset in frequency by $0.2\ f_c$, and 20 dB above thermal noise

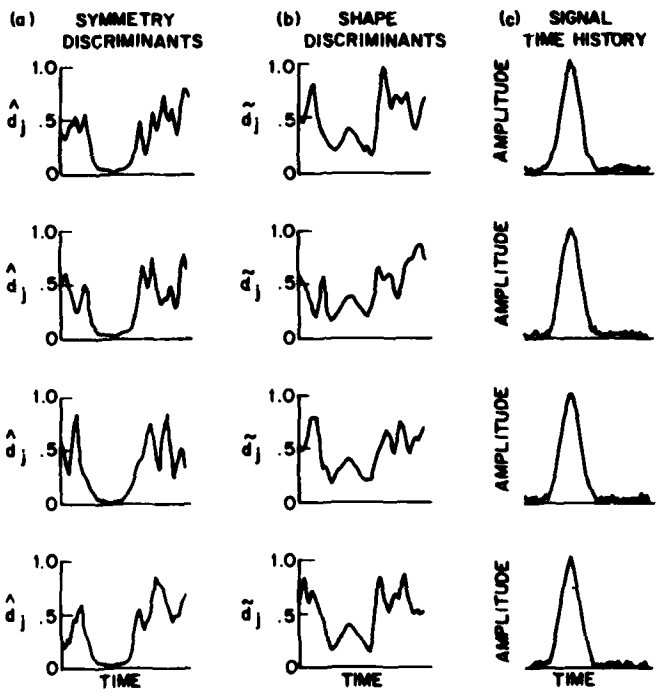

Fig. 19 — Time histories of discriminants and signals for four trials with a signal of bandwidth $f_c/5$ and 30 dB above thermal noise

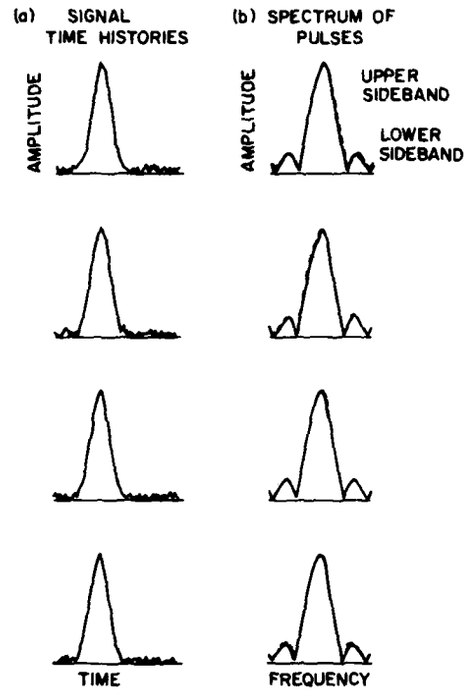

Fig. 20 — Time histories and spectrums of signals of bandwidths $f_c/5$ and 30 dB above thermal noise

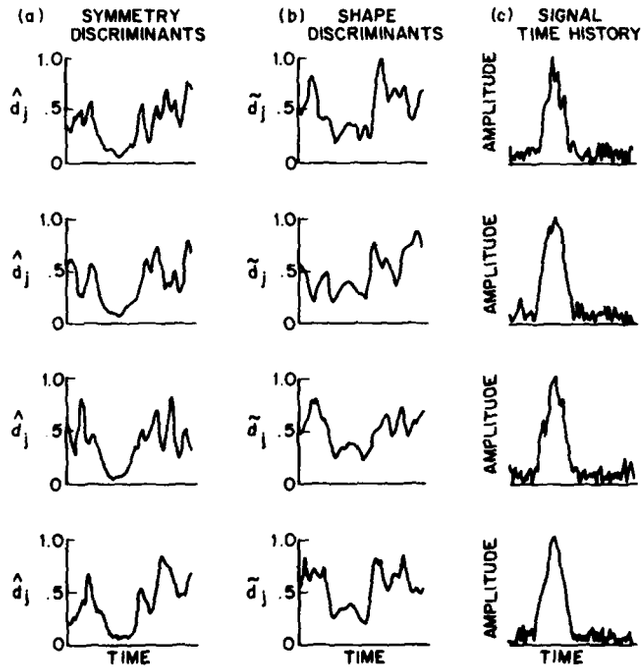

Fig. 21 — Time histories of discriminants and signals for four trials with a signal bandwidth $f_c/5$ and 20 dB above thermal noise

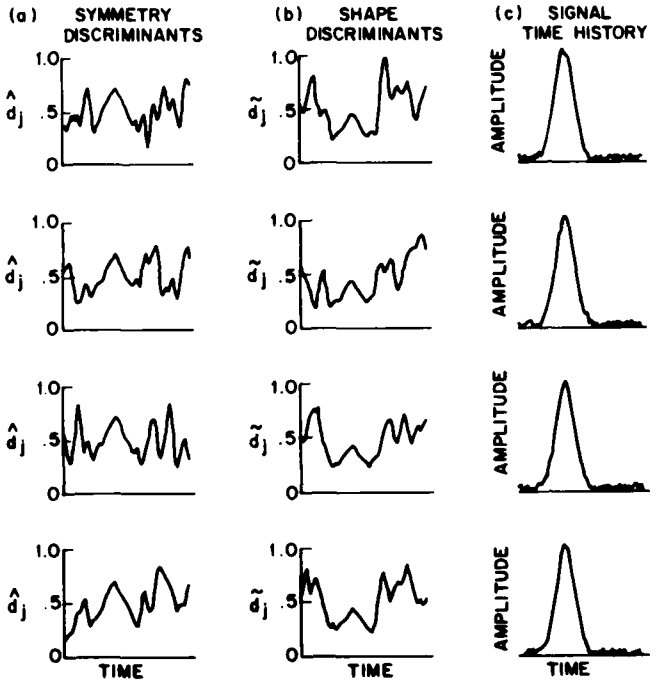

Fig. 22 — Time histories of discriminants and signals for four trials with a signal of bandwidth $f_c/5$, offset in frequency by 0.2 f_c, and 30 dB above thermal noise

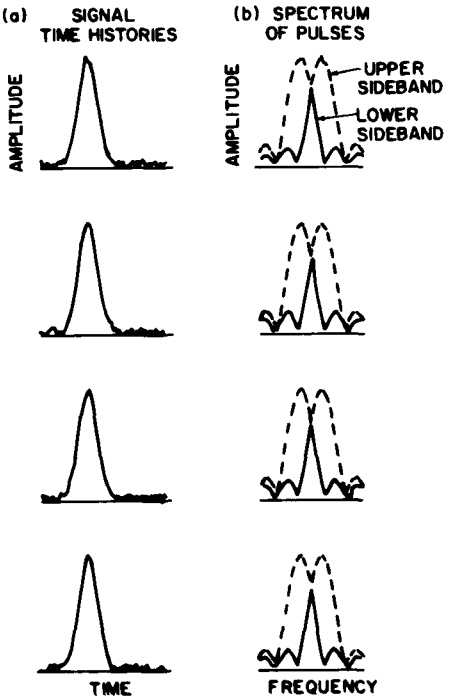

Fig. 23 — Time histories and spectrums of signals of bandwidths $f_c/5$, offset in frequency by 0.2 f_c and 30 dB above thermal noise

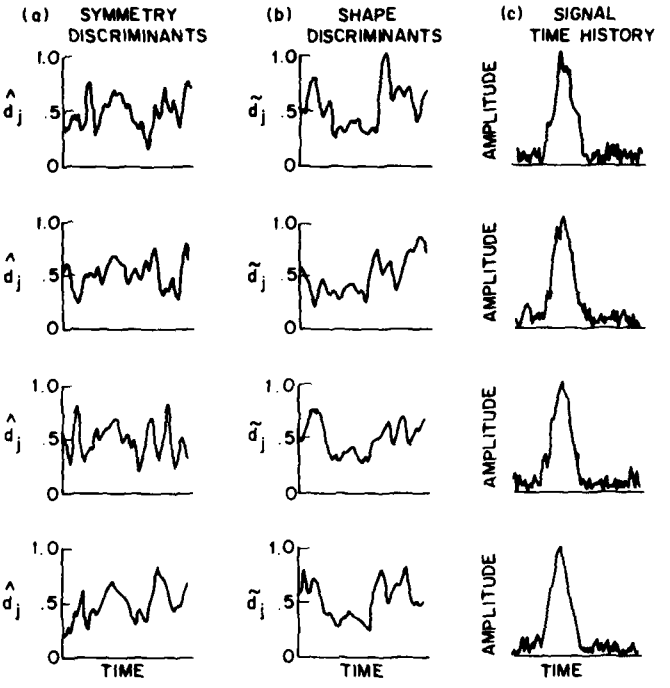

Fig. 24 — Time histories of discriminants and signals for four trials with a signal of bandwidth $f_c/5$, offset in frequency by 0.2 f_c, and 20 dB above thermal noise

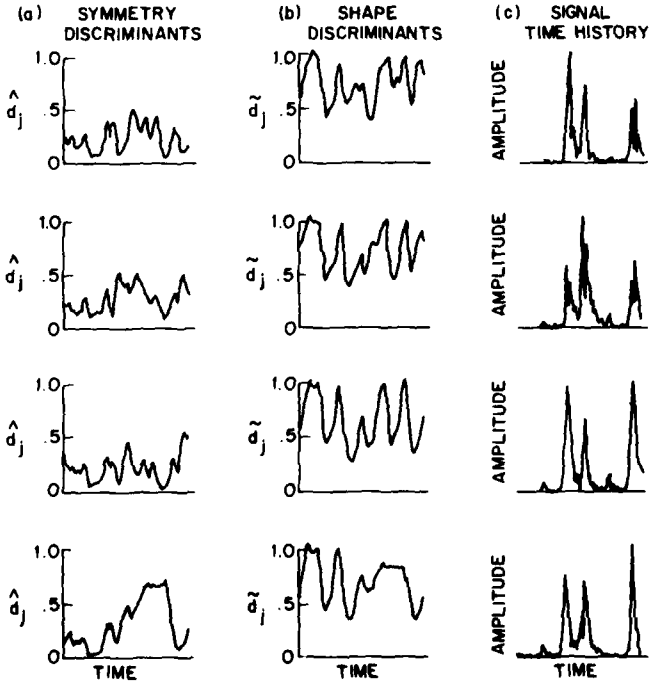

Fig. 25 — Time histories of discriminants and signals for four trials with a narrowband noise source equal in bandwidth to the receiver

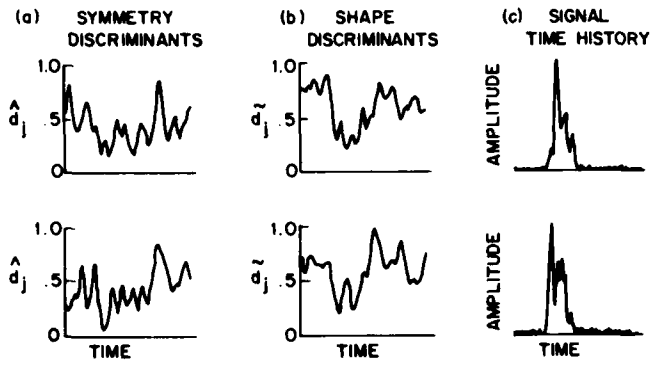

Fig. 26 — Time histories of discriminants and signals for two trials with a small region in time made up of a group of point scatters randomly distributed in range and amplitude

A very short duration (one fifth as long as the desired signal) RF pulse centered on the RF passband was passed through the receiver, and the results are shown in Figs. 13 and 15. The envelope of the received signal in Fig. 13c looks much like the return from a point target except for a little ringing of the filter on the back porch of the pulse. However, the test for a Gaussian shaped spectrum Fig. 13b shows that the spectrum is broad as indicated in Fig. 14b and the pulse would be declared interference. The test for symmetry in Fig. 13a looks targetlike because the short-duration RF pulse is centered on the carrier as shown by the spectrums in Fig. 14b. Figure 15 shows the same results as Fig. 13, except at a 20 dB S/N level.

The next interference studied was an RF pulse of short duration like the one described in Figs. 13 through 15 but now offset in frequency by $0.2 \times f_c$. The results are shown in Figs. 16 through 18 and for all practical purposes the results are the same as Figs. 13 through 15. The reason for this is that the spectrum of the signal is flat over frequency which is much larger than the passband and, consequently, the receiver passband is effectively controlling the received signal.

Next, a long-duration RF pulse centered on the receiver passband was passed through the receiver and the results are shown in Figs. 19 through 21. The envelope of the received pulse does not look like an echo from a point target because of its extent, as shown in Fig. 19c, and could probably be detected on this basis. However, the spectrum is narrower than the transmitted Gaussian shaped spectrum as shown in Fig. 20b and, consequently, the discriminant testing for shape in Fig. 19b does not indicate near zero which is a point target condition. The test on symmetry does exhibit a targetlike condition because the narrower spectrum is centered on the carrier. Figure 21 shows the same results as Fig. 19 except at a 20 dB S/N ratio.

Again we passed a long-duration RF pulse, but this time offset in carrier frequency, through the receiver. The results are shown in Figs. 22 through 24. The discriminant for spectral symmetry Fig. 22a now also shows the pulse is not point target like as well as the other discriminant in Fig. 22b. The offset in frequency as well as the narrower spectrum of the interference can clearly be seen in the spectrums shown in Fig. 23b. Figure 24 shows the same results except at 20 dB S/N.

We next looked at the effect of narrow bandwidth swept noise jamming. This was performed by sweeping the local oscillator through the narrow band noise out of the IF filter as shown in Fig. 1. The results are shown in Fig. 25. Some of the large amplitude spikes in the video shown in Fig. 25c look very targetlike. However, the discriminant in Fig. 25b shows the spectrum is not point targetlike and could be used to reject the pulses due to swept jamming. Most of the noise pulses, when they swept through, at some point produce a reasonably symmetric spectrum about the carrier and, therefore, the discriminants shown in Fig. 25a take on reasonably small values at the noise spikes.

We next looked at clutter type of returns which are characteristically modeled by the sum of many randomly distributed point scatters such as rain clutter. The results are shown in Fig. 26. The clutter return over a time frame is shown in Fig. 26c. The statistics should be noiselike if enough scatterers are used. It is doubtful that this is the case by observing Fig. 26, but more scatterers were not added because of the increase in cost. The discriminants in Fig. 26a and b do not exhibit targetlike characteristics but they do not look fully noiselike either due to not using enough scatterers. There appears to be a very strong dominant scatterer at the leading edge of the clutter in the trial shown at the bottom of Fig. 26.

Distributed Targets

We have found that the discriminants took on small values when point targets were present and at least one of the discriminants was not near zero when various types of interference was present. From this analysis, it appears that the discriminants could be useful in accepting point targets and rejecting interference. However, for distributed targets, the fine structure or spectrum of the pulse will be modified from a point target and we inquire as to how the results will be affected. We modeled the target with point scatterers randomly distributed over a time interval. The results for a target of an extent of 0.1 μs or 30 m (100 ft) long are shown in Figs. 27 and 28. The target extent is about one third of a pulse width. All but one of the trials yielded discriminant values nearly zero at the pulse. One trial shifted the spectrum a little as shown in Fig. 28b.

Trials using other target extents were performed and the results are shown in Figs. 29 and 30. For the most part, the discriminants were commensurable to what could be achieved with a point target. The case of the longer target extent (4/3 times the pulse width) in Fig. 30 is worse than the results in Fig. 29 for the target of 2/3 pulse widths.

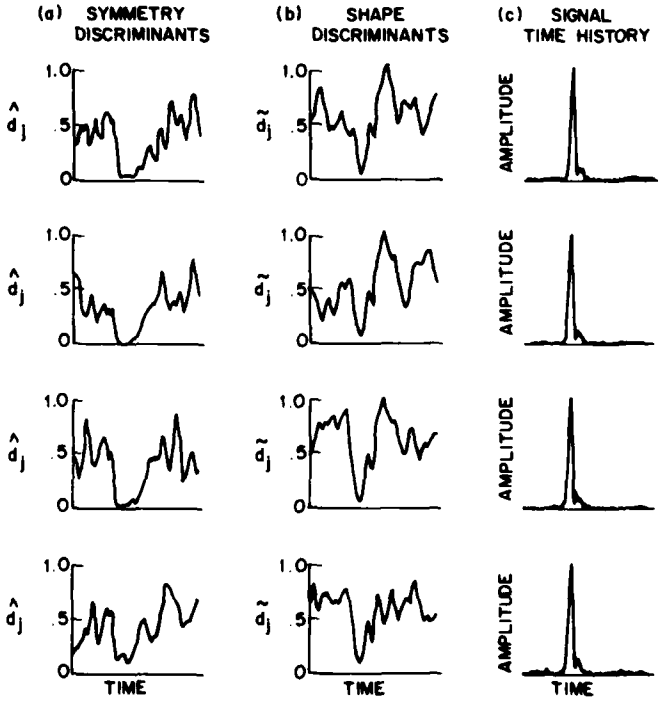

Fig. 27 — Time histories of discriminants and signals for four trials with a target of random scatters distributed over 0.1 μs at high $\approx$50 dB signal-to-noise ratio

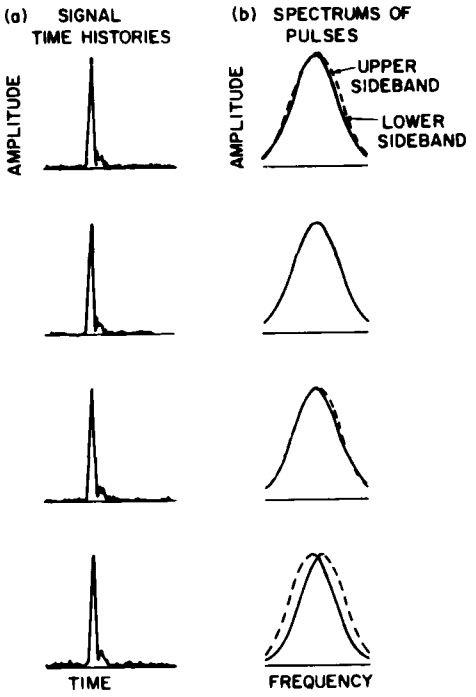

Fig. 28 — Time histories and spectrums of signals composed of a complex target of random scatters distributed over 0.1 μs at high $\approx$50 dB signal-to-noise ratio

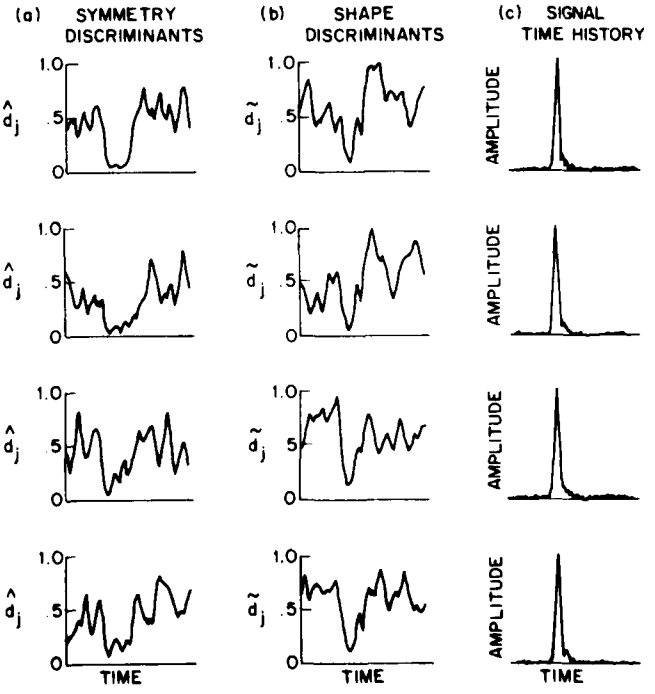

Fig. 29 — Time histories of discriminants and signals for four trials with a target of random scatters distributed over 0.2 μs at high $\approx$50 dB signal-to-noise ratio

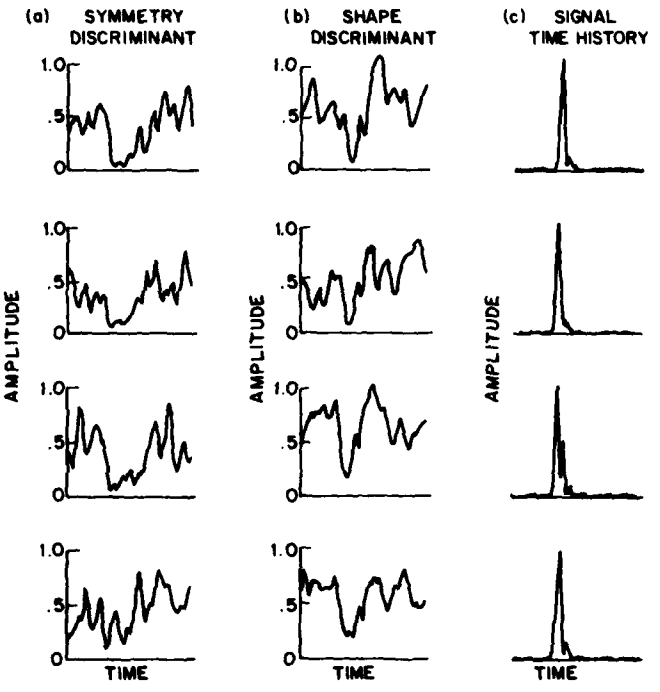

Fig. 30 — Time histories of discriminants and signals for four trials with a target of random scatters distributed over 0.4 μs at high $\approx$50 dB signal-to-noise ratio

One of the problems in this analysis is the availability of real target data. But from the simulated data, it appears that as long as the target is smaller than the pulse width, the discriminants do not on the average differ too much from that of a point target. If this is true for real targets, the discriminants appear useful in distinguishing between real targets and at least some types of interference.

SUMMARY

The purpose of this study was to determine if we could distinguish between target echoes and interference received by a radar on the basis of observing the fine structure of a pulse. Discriminants based on the magnitude of the spectral lines and properties of target echoes were formulated. This formulation alleviated the problems of not knowing phase and time-of-arrival which would have occurred in a time domain description. The study was conducted using a simulation of the superheteodyne single sideband synchronous receiver which was operated using a number of target and interference inputs based on models for excitations.

The basic results of the study demonstrated that probably good separation could be achieved between point target echoes and the kinds of interference studied. These results would tend to become worse as the target extent approached that of a pulse width. However, since the fine structure of a pulse is being used in the discrimination process, small changes in the signals or processes might make quite a difference. Consequently, it is difficult to draw strong conclusions on computer-generated data. Furthermore, because of cost we were not able to use a statistically significant set of samples. For strong conclusions to be drawn, a hardware implementation or at least data recordings would need to be made on a representative set of signals.

ACKNOWLEDGMENT

I would like to thank my colleague, Jeff Coleman, for aiding me in finding a good means of simulating a single sideband receiver and helping me to obtain a better understanding of the single sideband operations. Furthermore, the generally high interest he held and the resulting discussions during the course of this work were most helpful to me.

REFERENCES

[1] B.H. Cantrell, "Preliminary Results of Radar Environmental Mapping," NRL Report 8400, April 28, 1980.

[2] E. Norgaard, "The Phase-Shift Method of Single-Sideband Signal Reception," Proc. IRE **44** (12), 1735-1743, December 1956.


DAT
FILM